

Research Article

Biofunctionalized Magnetic Nanoparticles with Multiplex Touchdown PCR for Simultaneous and Rapid Detection/Identification of *Campylobacter jejuni* and *Campylobacter coli*

Pattarapong Wenbap ¹, Triwit Rattanarojpong ¹, Pongsak Khunrae ¹,
Taradon Luangtongkum ², Larry E. Erickson ³, Ryan R. Hansen ³,
and Pravate Tuitemwong ^{1,4}

¹Department of Microbiology, Faculty of Science, King Mongkut's University of Technology Thonburi, Bangkok 10140, Thailand

²Department of Veterinary Public Health, Faculty of Veterinary Science, Chulalongkorn University, Bangkok 10330, Thailand

³Tim Taylor Department of Chemical Engineering, Kansas State University, Manhattan, Kansas 66506, USA

⁴Food Safety Center, Institute for Scientific and Technological Research and Services, King Mongkut's University of Technology Thonburi, Bangkok 10140, Thailand

Correspondence should be addressed to Triwit Rattanarojpong; triwit.rat@mail.kmutt.ac.th
and Pravate Tuitemwong; pravate.tui@kmutt.ac.th

Received 30 June 2022; Revised 8 September 2022; Accepted 22 September 2022; Published 12 October 2022

Academic Editor: Mazeyar Parvinzadeh Gashti

Copyright © 2022 Pattarapong Wenbap et al. This is an open access article distributed under the Creative Commons Attribution License, which permits unrestricted use, distribution, and reproduction in any medium, provided the original work is properly cited.

The simple, accurate, and rapid detection of foodborne pathogens is essential for public health. Development of an immunomagnetic separation (IMS) multiplex touchdown PCR (IMS-multiplex TD-PCR) assay for simultaneous detection and distinguishing of *C. jejuni* and *C. coli* is reported herein. Polyclonal antibody (pAb) against multiepitope antigen (MEA) was conjugated to ferromagnetic nanoparticles (FMNs) to produce anti-MEA FMNs. Optimal anti-MEA FMNs loading yielded 26.7 μg of immunoglobulin G (IgG) molecules per mg of FMNs with an average size of 72 ± 9 nm, corresponding to an 83% rate of pAb conjugation. Anti-MEA FMNs (20 μg) for IMS captured culturable *C. jejuni* cells at 3.54×10^2 colony-forming unit (CFU)/mL in pure culture, while higher amounts (40 and 60 μg) reduced the recovery. The scanning electron microscope (SEM) analysis revealed the attachment of anti-MEA FMNs to target bacteria, forming aggregated cells and magnetic nanoparticles in ellipse-like shapes. The subsequent multiplex TD-PCR assay simultaneously detected and distinguished *C. jejuni* and *C. coli* at 10^4 CFU/mL in mixed culture and at 10^3 CFU/mL for each individual species. Furthermore, the limit of detection (LOD) of the IMS-multiplex TD-PCR assay was 10^4 CFU/g in spiked chicken breast samples. Specificity was 100% for both *C. jejuni* and *C. coli* as none of the amplicons were detected in control samples where *Campylobacter* was absent. This assay is able to detect and distinguish *C. jejuni* and *C. coli* simultaneously and is simple, accurate, and rapid with a time to result of 4 h without an enrichment step, making it a promising approach for rapid and culture-free detection of *Campylobacter* in chicken products.

1. Introduction

C. jejuni and *C. coli* are zoonotic pathogens and the cause of Campylobacteriosis. It is the most frequently reported foodborne illness in the EU with over 246,000 annual cases [1]. The Foodborne Diseases Active Surveillance Network (FoodNet) reported that overall incidence of infections

caused by *Campylobacter* was the highest (14.4 per 100,000 population) among all pathogens during 2020 [2]. The majority of infections are due to *C. jejuni* and *C. coli*, with an infectious dose of 500 CFU as reported by Black et al. [3]. However, *C. jejuni* have been reported to cause infections at as low as 360 CFU [4]. On average, two to five days after *C. jejuni* or *C. coli* infection, patients experience acute

watery or bloody diarrhea, cramps, weight loss, abdominal pain, and fever [5]. In rare cases, patients can develop neurological disorders such as Guillain Barre Syndrome [6]. *Campylobacter* spp. infections are prevalent around the world and have increased over the past decade [7]. For example, in Thailand it has been reported that *C. jejuni* and *C. coli* were present in 58% and 40% of diarrheal patients, respectively [8]. Chicken export is one of the important commodities of Thailand with annual export volume of 930 thousand metric tons [9, 10]. Given its global prevalence and the resulting detriments, it is necessary to continuously monitor food for the presence of these pathogens with accurate and rapid testing methods to ensure global food safety.

C. jejuni and *C. coli* are thermotolerant species and are flagellated spiral-rod Gram-negative bacteria with a single polar flagellum or bipolar flagella. Normally, these causative pathogens colonize in poultry gut and are cross-contaminated into poultry products during processing. A contaminated flock entering the slaughter line has high risk of cross-contamination into other chicken meat products by the end of the process. For example, it has been reported that 15% of neck skin samples from *Campylobacter*-free broiler flocks were contaminated by the end of processing and 25% (2/8) of those became contaminated after wet market processing [11]. The poultry plant environment and certain equipment surfaces such as defeathering machine, evisceration machine, floor, sink, conveyor belt, shackles, and broiler meat have been reported as sources of contamination as *C. jejuni* despite disinfection procedures [12].

In general, the gold standard method according to ISO 10272-1: 2017 [13] has been used for detection of *Campylobacter* spp. This conventional method is laborious and time-consuming, normally requiring 3–5 days to complete, while assay times of other reported detection methods were 0.5 to 3 h, as shown in Table 1. Alternatively, other methods available for detection of *Campylobacter* spp. include enzyme-linked immunosorbent assay (ELISA) methods, nucleic acid-based methods, and culture-based methods as well as fluorescence-based biosensing methods [14]. Unlike ELISAs, nucleic acid-based methods such as multiplex PCR or real-time PCR are widely used because of a superior limit of detection and high specificity [15]. Touchdown (TD)-PCR is an effective method for increased specificity in a multiplexed assay. However, reliable PCR methods also depend on pathogen capture and removal from the sample matrix.

Recently, magnetic nanoparticles (MNPs) with size ranging from 1 to 100 nm have been applied for various chemical and biological applications such as drug and gene delivery, biosensors, magnetic fluid hyperthermia (MFH), and magnetic resonance imaging (MRI) as well as immunomagnetic separation (IMS) [16]. Biofunctionalized magnetic nanoparticles, where nanoparticles are conjugated with biomolecules such as specific polyclonal or monoclonal antibodies, have been widely used for separation of target molecules in samples. Immunomagnetic separation using immunomagnetic beads (IMBs) has been effective for highly specific separation and enrichment of target bacteria [17]. Detection of a single target species of *C. jejuni* was reported with IMS using pAb-conjugated ferromagnetic nanoparticles

(FMNs) followed by PCR amplification of the *hipO* gene and detection using a lateral flow test strip assay. LODs were reported at 1 CFU/mL in pure culture and 10^1 – 10^2 CFU/mL in spiked poultry samples [18].

Single species detection using *C. jejuni*-*hipO* biomarker is highly problematic for food samples often contaminated with other *Campylobacter* species. In particular, *C. coli* contributes up to 25% of all *Campylobacter* gastroenteritis cases in some regions [5] and could go undetected with the current test. Species-level identification is also critical for epidemiological studies, such as identification of the source of a *Campylobacter* outbreak [23] and for understanding *Campylobacter* transmission routes [24] as well as clinical diagnosis. Recent surveillance studies revealed that patients infected with *C. jejuni* and *C. coli* have different demographic and clinical features [25], suggesting that these two species present different risk factors. Species-level distinction also informs that treatment options as antimicrobial susceptibility vary significantly between *Campylobacter* species. Antibiotic sensitivity is also different between *C. jejuni* and *C. coli*. Surveillance data revealed that *C. coli* strains are more resistant than *C. jejuni* to macrolide antimicrobials including azithromycin, erythromycin, and clindamycin [26]. Thus, choosing the right antibiotics is very significant for treatment of *Campylobacter* infections. Motivated by these factors, further development of a multiplexed IMS-based system to achieve rapid and simultaneous detection and distinction of *C. jejuni* and *C. coli* is essential.

High specificity of IMS can be provided by targeting CadF (*Campylobacter* adhesion to fibronectin) with a highly specific antibody covalently immobilized to FMNs. CadF is a highly conserved protein of *C. jejuni* and *C. coli* belonging to the outer membrane proteins superfamily and is responsible for binding to extracellular fibronectin [27, 28]. CadF is reported as having potential antigenicity [29, 30] and plays an important role in pathogenicity for *C. jejuni* and *C. coli* [31]. In our previous study, multi-epitope antigen (MEA), a chimeric protein composed of epitopes identified from *C. jejuni* CadF was produced as reported by Wenbap et al. [32]. MEA served as an antigen for eliciting rabbit immune system to produce a polyclonal antibody named anti-MEA pAb which recognizes both *C. jejuni* and *C. coli* through CadF binding [32]. In this study, the novelty of the IMS-multiplex TD-PCR assay reported here comes from the incorporation of highly specific MEA pAb for improved cell capture, combined with multiplexed PCR for rapid, sensitive detection, and distinction between *C. jejuni* and *C. coli*. Sensitive and simultaneous detection of both *Campylobacter* species is important to broaden the types of samples that are detectable with this approach, and distinction at the species level is important for epidemiological studies and for treatment decisions.

2. Materials and Methods

2.1. Biosafety Statement. The biosafety concern of this work was approved by the Institutional Biosafety Committee (IBC) with the approval number KMUTT-IBC-2019-087.

TABLE 1: A variety of rapid detection methods for detection of *Campylobacter* spp.

Detection methods	Target bacteria	Assay time (h)	References
Culture-based method	<i>C. jejuni</i> and <i>C. coli</i>	≥5 days	[13]
IMS–loop–mediated isothermal amplification method	Thermophilic <i>Campylobacter</i> sp.	1.5	[19]
IMS combined with lateral flow chromatographic test (LFT) assay	<i>C. jejuni</i>	3	[18]
Broth enrichment and rplD–LAMP assays	<i>C. jejuni</i> and <i>C. coli</i>	48	[20]
Silica nanoparticle enhanced dot blot DNA biosensor	<i>Campylobacter</i> spp.	24	[21]
Fluorescence immunochromatography (FIC) assay	Thermophilic <i>Campylobacter</i> sp.	0.5	[22]
IMS–multiplex TD–PCR assay	<i>C. jejuni</i> and <i>C. coli</i>	4	This study

2.2. *Microorganisms and Growth Media.* Target and nontarget bacteria were kindly gifted by the Food Safety Center (KMUTT, Thailand) and are listed in supplementary Table S1. *Campylobacter* spp. were cultured on modified cefoperazone charcoal deoxycholate agar (mCCDA) (Oxoid, Thermo Fisher Scientific) and incubated at 41.5°C for 48 h under microaerophilic condition (O₂ 5% + CO₂ 10% + N₂ 85%). Non-*Campylobacter* species were cultured on Tryptic Soy Agar (TSA) plate and incubated at appropriate growth conditions.

2.3. *Preparation of Amino Functionalized Ferromagnetic Nanoparticles (FMNs).* The FMNs were synthesized by polyol technique [18, 33]. Briefly, 2 g of iron (III) chloride hexahydrate (FeCl₃·6H₂O) were added into 40 mL ethylene glycol ((CH₂OH)₂), stirred until the solution turn to yellow color. After that, 6 g of sodium acetate (CH₃COONa), 1.6 g of sodium hydroxide (NaOH), and 20 mL of ethylenediamine (C₂H₄(NH₂)₂) were added into the solution and stirred for 30 min followed by autoclaving at 121°C for 2 h, for 3 cycles. The amino–FMNs obtained from autoclaving were then separated from solution by a magnet followed by washing in an ultrasonic bath sonicator for 3 times in distilled water and 95% ethanol, respectively. The amino–FMNs were placed in a beaker wrapped with aluminum foil and dried at 50°C for 24 h, crushed with a mortar, and stored in amber glass reagent bottle. Subsequently, the crushed amino–FMNs were resuspended in 1× phosphate-buffered saline (PBS; 137 mM sodium chloride (NaCl), 2.7 mM potassium chloride (KCl), 10 mM disodium phosphate (Na₂HPO₄), and 1.8 mM potassium dihydrogen phosphate (KH₂PO₄), pH 7.4) and sonicated for 48 h prior to use.

2.4. Surface Modification and Conjugation of Anti-MEA Polyclonal Antibody to Amino–FMNs

2.4.1. *Glutaraldehyde Surface Modification.* To provide immunological activity for the FMNs particles, the FMNs particles were modified with 2.5% glutaraldehyde in 1× PBS prior to the antibody conjugation. Briefly, 100 mg of amino–FMNs were resuspended into 50 mL 1× PBS containing 2.5% glutaraldehyde. The amino–FMNs mixture was stirred on a magnetic stirrer for 2 h at room temperature. Subsequently, amino–FMNs were separated, washed with 1× PBS, and resuspended in 50 mL of 1× PBS to final con-

centration of 2 mg/mL. The modified FMNs were stored at 4°C until use.

2.4.2. *Conjugation of Anti-MEA Polyclonal Antibody to the Modified FMNs.* Immunological activity of the FMNs were provided by conjugation of *C. jejuni*- and *C. coli*-specific pAb (anti-multiepitope antigen (MEA) pAb) which were prepared as described in our previous work [32]. The optimal initial concentration of antibody for conjugation was investigated. The different concentrations of anti-MEA pAb solution were prepared by PBS–double dilution (1:20, 1:40, 1:80, 1:160, 1:320, and 1:640), which resulted in concentrations of 264.0, 127.7, 64.0, 30.4, 18.5, and 15.4 µg/mL, respectively. Each diluted antibody solution (500 µL) was incubated with 1 mg of modified FMNs at 18°C overnight with shaking at 150 rpm. Each batch of FMNs with IgG-conjugated (anti-MEA FMNs) and unconjugated FMNs (control FMNs) prepared from different conditions were separated by a magnet, washed with sterilized 1× PBS, and incubated overnight with 5% bovine serum albumin (BSA)–PBS blocking solution at 4°C with gentle shaking at 150 rpm. Each batch of anti-MEA FMNs and control FMNs were recovered and washed with 1× PBST (PBS with 0.05% Tween) and 1× PBS, respectively. Finally, it was resuspended with 1 mL 1× PBS to receive the final concentration of 1 mg FMNs/mL and stored at 4°C prior to use. Each conjugation was performed in triplicate. The remaining antibody after each conjugation was quantified by Lowry assay and was subtracted from the initial concentrations to calculate the concentration of anti-MEA pAb loading on FMNs. BSA standard solutions were prepared at different concentrations varying from 200 to 1000 µg/mL to build the standard curve (Supplementary Figure S1) by Lowry assay at 750 nm using microplate reader. The loadings of anti-MEA pAb on FMNs were calculated as follows:

$$\text{The loading of antibody } (\mu\text{g}) \text{ on } 1 \text{ mg FMNs} = (C_0 - C_1) \times 0.5 \text{ mL}, \quad (1)$$

where C_0 is the initial concentration of antibody solution before conjugation (µg/mL) and C_1 is the remaining concentration of antibody solution after conjugation (µg/mL).

2.5. *Analysis of Capture Efficiency and Optimization of Amount of Anti-MEA FMNs for Detecting Culturable *C. jejuni* in Immunomagnetic Separation (IMS) System.* Each

batch of anti-MEA FMNs and control FMNs were used in IMS system to determine immunological activity for capturing of target bacterial cells. In this study, *C. jejuni* was the representative organism for the analysis of capture efficiency. Briefly, *C. jejuni* suspension turbidity at optical density of 600 nm (OD_{600}) was adjusted to 1.0 which is equivalent to 10^8 CFU/mL and diluted to 10^6 CFU/mL by $1\times$ PBS. Subsequently, $20\ \mu\text{g}$ of each batch of anti-MEA FMNs was mixed thoroughly with *C. jejuni* suspension. The mixtures were incubated at 37°C for 1 h with shaking at 150 rpm. The *C. jejuni*-FMNs complexes were recovered by a magnetic concentrator followed by washing with 1 mL of $1\times$ PBST and $1\times$ PBS, respectively. Thereafter, the washed FMNs were resuspended into $100\ \mu\text{L}$ $1\times$ PBS, cultured on mCCDA plate and incubated at 41.5°C for 48 h under micro-aerophilic condition. Typical colonies of *C. jejuni* which appeared as white-curved like fried-egg colonies were enumerated. Capture efficiency of each anti-MEA FMNs was determined by the number of recovered cells that appeared on an mCCDA plate and expressed as CFU/mL detected.

The amount of anti-MEA FMNs was optimized for IMS system. Three batches of anti-MEA FMNs giving high capture efficiency which were obtained from the previous experiment were used at 10, 20, 40, and $60\ \mu\text{g}$ for the IMS system. Each of anti-MEA FMNs was mixed with a *C. jejuni* suspension at the same concentration followed by incubation at 37°C for 1 h with shaking at 150 rpm. Washing and culturing steps were performed as described above. The amount of anti-MEA FMNs with the highest recovered CFU/mL was chosen for the next experiments. Experiments were done in triplicate.

2.6. Scanning Electron Microscope (SEM) Analysis. To observe the microstructure and morphology of the anti-MEA FMNs after binding to target bacterial cells, SEM analysis was performed. Briefly, the FMNs complexes recovered from IMS system were subjected to the protocols of fixation and dehydration before SEM analysis. The FMNs complexes ($20\ \mu\text{g}$) were incubated with 1 mL $1\times$ PBS (pH 7.4) on ice for 15 min and magnetically separated or alternatively, centrifuged at 5000 rpm for 5 min at 4°C . This step was done 3 times. Samples were then fixed (2.5% glutaraldehyde in $1\times$ PBS) and incubated at 4°C for 12h followed by washing with $1\times$ PBS and $0.5\times$ PBS. To eliminate salts and water in samples prior to being observed by SEM, the complexes were dehydrated by incubating with a series of ethanol solutions as follows: 25% (20 min), 50% (20 min), 75% (12h), 90% (20 min), and 99.5% absolute ethanol (12 h). Each step was carried out at 4°C . Finally, the complexes were stored in absolute ethanol at 4°C . The SEM analysis was conducted at the Synchrotron Light Research Institute (Thailand).

2.7. Polymerase Chain Reaction (PCR) Procedure

2.7.1. Bioinformatic Analysis and Design of PCR Primers. To design effective PCR primers, bioinformatic analysis was carried out according to the protocol described by Abd-Elsalam [34]. Ninety-five and twenty sequences of *C. jejuni*-*hipO* and *C. coli*-*ask* genes, respectively, were retrieved for the

National Center for Biotechnology Information (NCBI) site [35]. To identify consensus sequence of *hipO* and *C. coli*-*ask* genes, multiple sequence alignment (MSA) analyses were performed using the SnapGene Viewer software with a threshold of 0.9. Thereafter, conserved and unique regions of each consensus sequence were selected to be used as PCR primers. Each primer (19–22 mers) is shown in Table 2 and was identified according to their highest conservation of regions and synthesized at Bioneer (Korea). The designed primers were analyzed for their properties, self-dimer forming, and PCR reaction by Oligo Analysis Tool [36]. Specificities of each primer pair were checked by primer-BLAST online tool [37].

2.7.2. Optimization of Multiplex Touchdown PCR Assays. The concentrations of primers were optimized to avoid competition in the multiplex detection.

Multiplex TD-PCR assay was performed using 3 primer pairs as shown in Table 2. Primer pairs FW226–RV699 and FW346–RV529 were optimized at different concentrations varying from $0.1\ \mu\text{M}$ to $0.5\ \mu\text{M}$ with fixed concentration ($0.2\ \mu\text{M}$) of C412F–C1288R [38]. To prepare bacterial DNA templates of *C. jejuni* ATCC 33560 and *C. coli* NTCC 11353, bacterial cells were suspended in nuclease-free water (HyClone™ Molecular Biology Grade Water, Cytiva) and boiled for 10 min. The supernatants were collected, the DNA concentration was measured by Nanodrop™ Lite Spectrophotometer (Thermo Fisher Scientific, USA) before use, and the DNA templates were stored at -20°C . The total amount of DNA template (100 ng each) did not exceed $5\ \mu\text{L}$ per PCR reaction. The multiplex TD-PCR reaction was performed in a total volume of $20\ \mu\text{L}$ in a T100 Thermal cycler (Bio-Rad, USA) with the touchdown PCR condition (Table 3). The mPCR mixture included $10\ \mu\text{L}$ of ($2\times$) PCR i-Taq Master mix Solution (iNtRON Biotechnology, Korea); $2.8\ \mu\text{L}$ of an optimal mixed primer; $0.4\ \mu\text{L}$ of C412F, C1288R, FW346, and RV529; $0.6\ \mu\text{L}$ of FW226 and RV699 ($10\ \mu\text{M}$ each); $5\ \mu\text{L}$ of DNA template sample; and $2.2\ \mu\text{L}$ of nuclease-free water. This optimal TD-PCR condition was applied for IMS-multiplex TD-PCR assay.

After thermal cycling reaction was completed, $5\ \mu\text{L}$ of PCR product or 100 bp+3 K DNA ladder (ExcelBand, SMO-BIO, Taiwan) were mixed with $1\ \mu\text{L}$ of $6\times$ FluroDye DNA Fluorescent Loading Dye (SMOBIO, Taiwan) and visualized by 1.8% agarose gel electrophoresis in $1\times$ Tris-Borate-EDTA (TBE) buffer (Thermo Scientific, USA) using Mini Run Gel Electrophoresis System (Life Science, USA). The agarose gel was visualized and imaged under SafeViewer Blue Light Transilluminator (TT-BLT-470; Hercuvan, UK).

2.8. Immunomagnetic Separation (IMS)-Multiplex TD-PCR Assays. The anti-MEA FMNs were used as the capture agent in the IMS system. First, $20\ \mu\text{g}$ of anti-MEA FMNs were mixed to 1 mL in either pure culture or artificial contaminated chicken meat homogenates and subsequently incubated at 37°C for 1 h with shaking at 150 rpm. After that, the reaction tubes were placed in magnetic separation racks for 5 min to separate the complexes, then the supernatant was discarded. The recovered complexes were washed with 1 mL $1\times$ PBST and $1\times$ PBS, respectively. Second, to prepare

TABLE 2: Primers used in multiplex TD-PCR assay for detection of *Campylobacter* spp.

Target gene	Primer name	Sequence (5'-3')	Tm (°C)	GC (%)	Size (bp)	Target bacteria	References
<i>16s rRNA</i>	C412F	GGATGACACTTTTCGGAGC	62.7	52.6	816	<i>Campylobacter</i> spp.	[38]
	C1288R	CATTGTAGCACGTGTGTC	56.5	50.0			
<i>hipO</i>	FW226	GATATGGATGCTTTGCCTT	56.3	42.1	474	<i>C. jejuni</i>	In this study
	RV699	GCTTACAACCTGCTGAATTTTG	57.3	38.1			
<i>ask</i>	FW346	GACACTCAAGCAATCACCA	58.7	47.4	184	<i>C. coli</i>	In this study
	RV529	CTCCATCCACATCGGTATAAA	58.0	42.9			

TABLE 3: The multiplex touch down PCR conditions.

Steps	Temperature and time of amplification cycle	Number of cycles
Initial denaturation	94°C for 2 min	1
	94°C for 30 s, 65°C for 15 s, 72°C for 40 s	3
	94°C for 30 s, 63°C for 15 s, 72°C for 40 s	3
	94°C for 30 s, 61°C for 15 s, 72°C for 40 s	3
	94°C for 30 s, 59°C for 15 s, 72°C for 40 s	3
Denaturation, annealing and extension	94°C for 30 s, 57°C for 15 s, 72°C for 40 s	3
	94°C for 30 s, 55°C for 15 s, 72°C for 40 s	9
	94°C for 30 s, 53°C for 15 s, 72°C for 40 s	15
	72°C for 5 min	1
Final extension	12°C for 5 min	1

the DNA templates for multiplex TD-PCR assay, the recovered complexes were resuspended with 50 μ L nuclease-free water and boiled for 10 min to allow the extraction of genomic DNA. After boiling, it was subsequently refrigerated at 4°C for 5 min and then placed in the magnetic separation rack to separate the immunomagnetic beads, and the supernatant of crude DNA was collected. Thereafter, 5 μ L of crude DNA was subjected to the multiplex TD-PCR assay protocol described above. The supernatant of crude DNA was stored at -20°C prior to use.

2.9. Determination of Sensitivity and Specificity of IMS-Multiplex TD-PCR Assays

2.9.1. Sensitivity of IMS-Multiplex TD-PCR Assay in Pure Cultures. LODs of the IMS-multiplex TD-PCR assay were determined for the target bacteria in both pure and mixed cultures. For pure cultures, each series of 10-fold PBS diluted bacterial suspension of *C. jejuni* and *C. coli* were prepared at different concentrations ranging from 10^0 to 10^7 CFU/mL. To prepare the mixed culture, equal volumes of *C. jejuni* and *C. coli* (10^8 CFU/mL) suspension were pooled together at ratio 1:1, and a series of 10-fold PBS diluted bacterial suspensions was carried out to receive the final concentration of 10^0 to 10^7 CFU/mL. Thereafter, each series of single pure or mixed culture was subjected to the IMS-multiplex TD-PCR assay as described above. Additionally, IMS-plating assay was performed for mixed cultures to observe the number of culturable captured target cells. Each set of experiments was done in triplicate.

2.9.2. Specificity of IMS-Multiplex TD-PCR Assays. The range of inclusive ($n = 50$) and exclusive ($n = 28$) strains (supplementary Table S1) in pure form was used for specificity study. A total of 50 *Campylobacter* spp. strains including 4 reference strains and 46 chicken isolates were cultured and PBS-diluted to receive the final concentration of 10^3 CFU/mL for testing with IMS-multiplex TD-PCR assay. The exclusivity test was performed as the following. A mix of 3 strains of bacteria in the same genus (10^6 CFU/mL each) was prepared as genus cocktails (supplementary Table S2), and thereafter, it was subjected to the IMS-multiplex TD-PCR assay.

2.9.3. Effect of Food Sample Matrices on IMS-Multiplex TD-PCR Assay and Its Sensitivity. To determine the LOD of IMS-multiplex TD-PCR assay for *C. jejuni* and *C. coli* in biological samples ($n = 10$), chilled chicken breast products were purchased from a supermarket in Bangkok, Thailand. It was tested for the natural presence of *Campylobacter* spp. by both conventional gold standard method ISO 10272-1 [13] and IMS-multiplex TD-PCR assay. To prepare a series of mixed cultures, cell suspension containing *C. jejuni* and *C. coli* at ratio 1:1 (10^8 CFU/mL each) was diluted with 1 \times PBS to prepare an approximate concentration of 10^1 to 10^7 CFU/mL each. *Campylobacter*-free samples were artificially contaminated as follows: Ten g of small pieces of chicken breast sample were aseptically transferred into stomacher bag and spiked with 1 mL of a series of mixed cultures (10^1 to 10^8 CFU/mL) to receive the final concentration of 10^0 to 10^7 CFU/g for each of *C. jejuni* and *C.*

coli. The contaminated samples were added with 90 mL 1× PBS then homogenized at low speed for 30 sec. Thereafter, 1 mL of each homogenate was transferred to 1.5 mL microcentrifuge tube, and 20 μg of anti-MEA FMNs was added for the IMS–multiplex TD–PCR assay. Experiment was done in triplicate.

3. Results and Discussion

3.1. Synthesis of Amino-FMNs and Conjugation of Anti-MEA Polyclonal Antibody. The amino-FMNs synthesized by the polyol technique yielded dark-brown precipitates in solution. After drying and crushing, the amino-FMNs displayed magnetic properties as it was separated by a magnet (Supplementary Figure S2). During the synthesis reaction, ethylenediamine was used as a source of amine group which was afterward reacted with glutaraldehyde. Magnetization curves and magnetic hysteresis loops of amino-FMNs synthesized by polyol technique have been previously reported and characterized between ferromagnetism and superparamagnetism with a saturation magnetization (M_s) of about 48 emu/g, remanence (M_r) of 1.7 emu/g, and coercivity (H_c) of 23.5 Oe [33]. The amino-FMNs were treated with glutaraldehyde and, thereafter, conjugated with anti-MEA pAb specific to *C. jejuni* and *C. coli*. Glutaraldehyde was used as crosslink agent providing aldehyde groups (–CHO) reactive towards amino-FMNs. Interaction of aldehyde and amino (–NH₂) groups leads to formation of imine bonds (C=N) resulting in FMNs with a free aldehyde group available for antibody conjugation as illustrated in Figure 1. FMN surface modification with 5% glutaraldehyde was evaluated using Synchrotron Fourier Transform Infrared (FTIR) spectroscopy by Sukprasert et al. [39], who confirmed the availability of aldehyde groups for antibody attachment while minimizing nanoparticle aggregation at this concentration.

Subsequently, conjugations of anti-MEA pAb to glutaraldehyde-treated FMNs were carried out at various initial pAb concentrations. The results showed that higher initial pAb concentrations resulted in higher pAb loading on FMNs. The pAb loading gradually decreased from 45.2 to 2.8 $\mu\text{g}/\text{mg}$ FMNs as initial pAb concentrations were diluted from 1:20 to 1:640, respectively (Figure 2). Considering the significant cost of antibody, the percentages of each pAb conjugation was also compared. The percentages of pAb conjugation reached a maximum of 83% by incubation with anti-MEA pAb at 1:80 dilution (64.0 $\mu\text{g}/\text{mL}$) which yielded the pAb loading at 26.7 μg and was slightly decreased to 82% and 71% at 1:160 and 1:320 dilutions, respectively. Controlling the ratio of modified-FMNs and polyclonal antibody as well as all parameters including temperature and incubating shaking for conjugation was critical for reproducibility. Dot blot analysis was used to confirm results of each batch of pAb loading on FMNs; data are shown in supplementary Figure S4.

An optimal biotinylated pAb amount of 60 μg per 1 mg streptavidin-conjugated magnetic nanoparticles for capturing *Vibrio parahaemolyticus* have been reported [40]. In this study, the use of higher and lower pAb concentrations

resulted in lower percent conjugation. Although incubation of FMNs with pAb at 1:20 dilution yielded the highest pAb loading at 45.2 μg , the percentage of pAb conjugation was only 34%. This implies that reactive sites on FMNs become saturated or inaccessible at higher pAb levels, resulting in excess pAb in the solution. Although there were differences in pAb loading and percentage of pAb conjugation, each batch of anti-MEA FMNs from different conjugation conditions was investigated for the capability of capturing target bacterial cells.

3.2. Capture Efficiency of Anti-MEA FMNs in IMS System. *C. jejuni* was subjected to each batch of anti-MEA FMNs to determine its capture efficiency for IMS. As the pAb loading increased from 2.8 to 26.7 μg per 1 mg FMNs, the capture levels increased and reached the highest captured CFU value of 3.9×10^2 CFU/mL at 26.7 μg as shown in Figure 3. Hypothetically, the anti-MEA FMNs with the highest pAb loading was expected to capture more target cells because more antibody should have provided more target antigen-binding sites. Surprisingly, the capture levels decreased when pAb loading was increased from 26.7 to 45.2 $\mu\text{g}/\text{mg}$ FMNs. The control FMNs were not able to capture target bacterial cells because they were not functionalized with antibodies. This also confirmed the immunological activity of the anti-MEA pAb towards *C. jejuni* and *C. coli* (data not shown). Reduction of capture with higher antibody loading has been reported elsewhere, including in Zhou et al. where increasing antibody loading from 300 to 1200 μg decreased capture [41]. There is a possibility that excessive pAb molecules immobilized onto FMNs could cause crowding that sterically blocks a portion of antigen-binding sites. The nonspecific coupling of amino groups to FMNs through aldehyde–amino group reactions could also result in pAb coupling near the antigen-binding site, leading to reduction of target-binding activity. Also, captured cells may lose their viability and culturability during the IMS process, which could also be the cause of larger error that was observed during plating assays to determine CFU/mL (Figure 3). According to percentage of pAb conjugation, three batches of anti-MEA FMNs resulting in pAb loading at 38.0, 26.7, and 13.2 μg per mg FMNs, respectively, were economically feasible and chosen for further optimization.

3.3. Optimization of Anti-MEA FMNs Concentration for Capture and IMS. *C. jejuni* was used as a representative target bacteria in this experiment. Each batch of anti-MEA FMNs from 1:40, 1:80, and 1:160 dilutions was investigated for IMS at varied concentrations of 10, 20, 40, and 60 $\mu\text{g}/\text{mL}$. The results revealed that using 20 μg of 26.7 μg -coated pAb FMNs reached the highest amount of recovered *C. jejuni* cells at 3.54×10^2 CFU/mL, as determined by plating. Similar results could be obtained by using the same amount of 13.2 μg -coated pAb FMNs, as shown in Figure 4. However, adding higher concentrations of anti-MEA FMNs (40 and 60 $\mu\text{g}/\text{mL}$) reduced the capture efficiency for *C. jejuni*. It is likely that these higher concentrations result in large number of magnetic beads to attach to target cells and form a tight complexes [42] which would

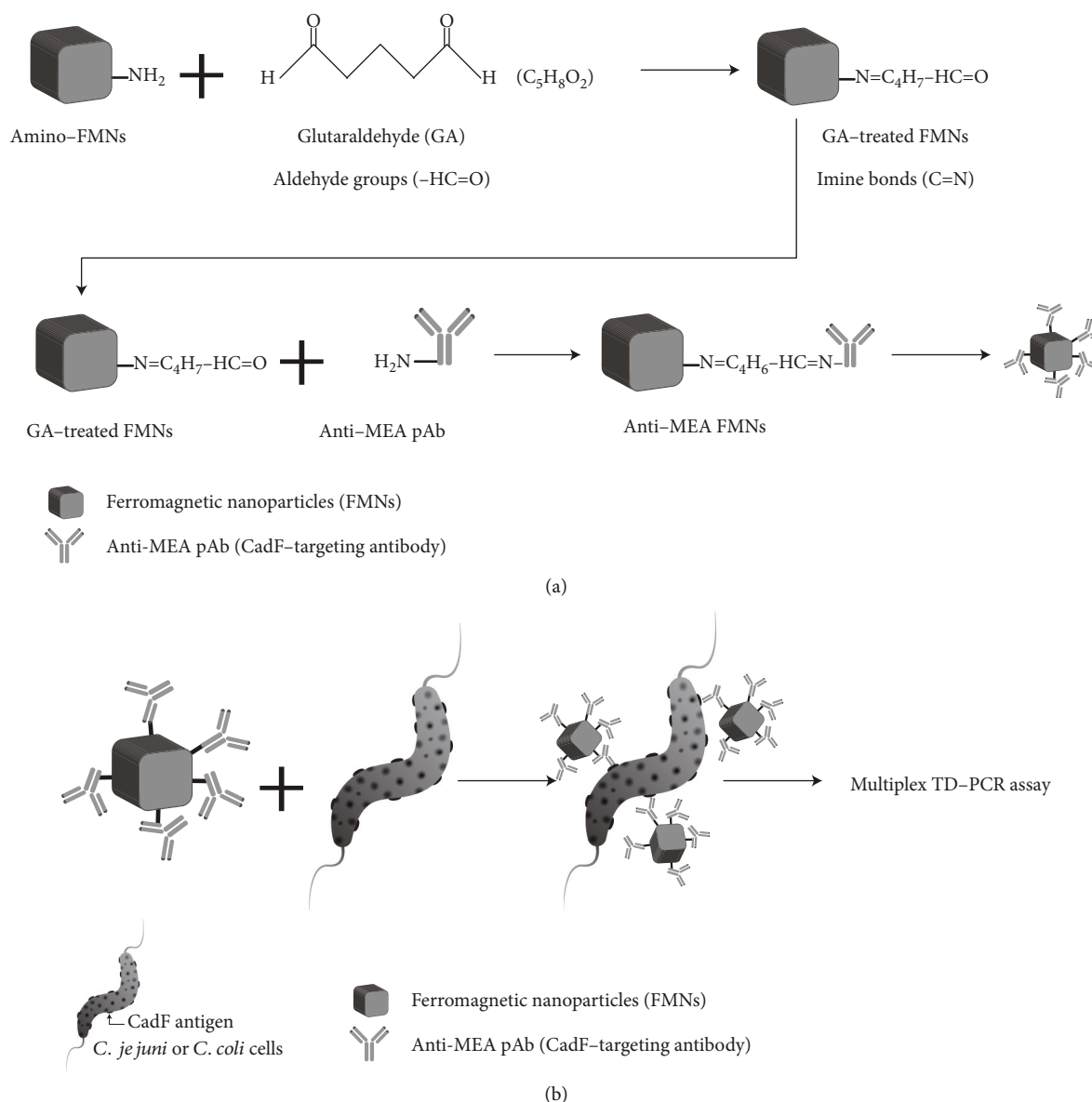


FIGURE 1: Schematic illustrating the functionalization of anti-MEA FMNs (a) and the overall procedure of IMS-multiplex TD-PCR assay to detect *C. jejuni* and *C. coli* cells (b).

compromise cell viability and lead to lower CFU/mL when plating on media. Therefore, $20 \mu\text{g}$ of anti-MEA FMNs from a batch of 1:80 dilution was optimum and chosen for further experiments. At this condition, anti-MEA FMNs were reproducible in lab-scale production. Further investigation of batch-to-batch reproducibility during large-scale production is necessary for future production.

3.4. SEM of Anti-MEA FMNs and Binding of Anti-MEA FMNs to *C. jejuni* and *C. coli* Cells. Scanning electron microscope (SEM) images revealed the cubic shape of amino-FMNs, and the size of particles was found to be $72 \pm 9 \text{ nm}$ (Figure 5(a)). Steaming in an autoclave at 121°C , gave uniform size with cubic shape nanoparticles. The characteristics corresponded well to that of the previous studies [18, 33, 39]. The average size of FMNs, however, was slightly larger than

the size ($43 \pm 9 \text{ nm}$) reported by Songvorawit et al. (2011). The anti-MEA FMNs formed aggregates as shown in Figures 5(a) and 5(b). Aggregation may be caused during the antibody conjugation step as anti-MEA pAb contains multiple amino groups in the form of lysine residues that can couple with multiple aldehyde groups (-CHO) available on glutaraldehyde-treated FMNs [39]. Aggregation may also occur during the desalting and dehydration steps required for SEM analysis. Particles size may also affect capture efficiency. There are various reports using immunomagnetic beads with different sizes in the range of 10 nm up to $2.8 \mu\text{m}$. However, the highest recovery of *Salmonella* cells was received by using 100 nm IMBs, and reductions in recovery could be affected by higher IMB sizes (500 and 1000 nm) [43].

C. jejuni or *C. coli* cell-FMNs complexes were also observed under SEM after IMS. Interestingly, SEM images

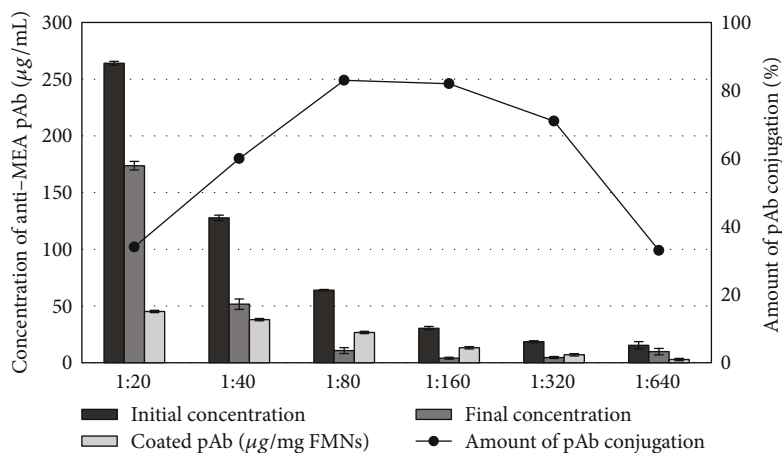


FIGURE 2: Amount of pAb conjugation and loading of anti-MEA pAb on FMNs.

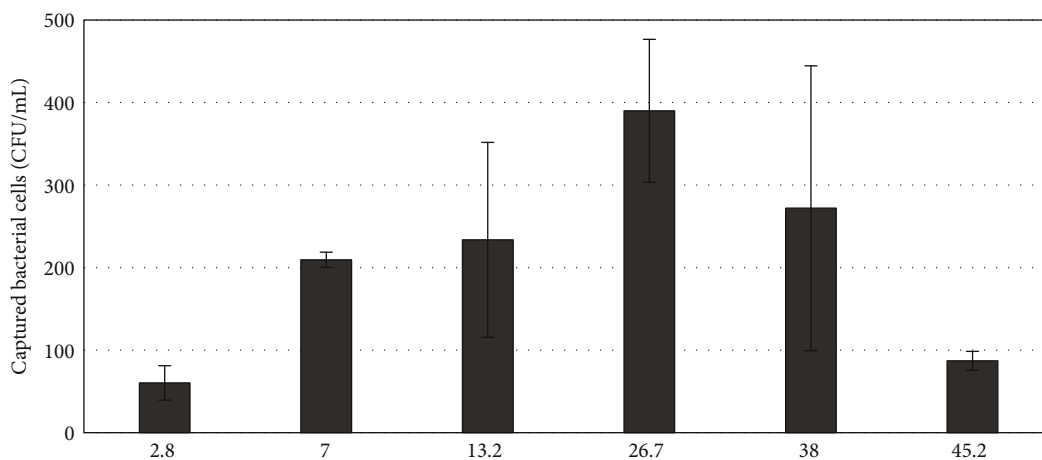


FIGURE 3: Capture levels of *C. jejuni* ATCC 33560 for different anti-MEA loading on FMNs.

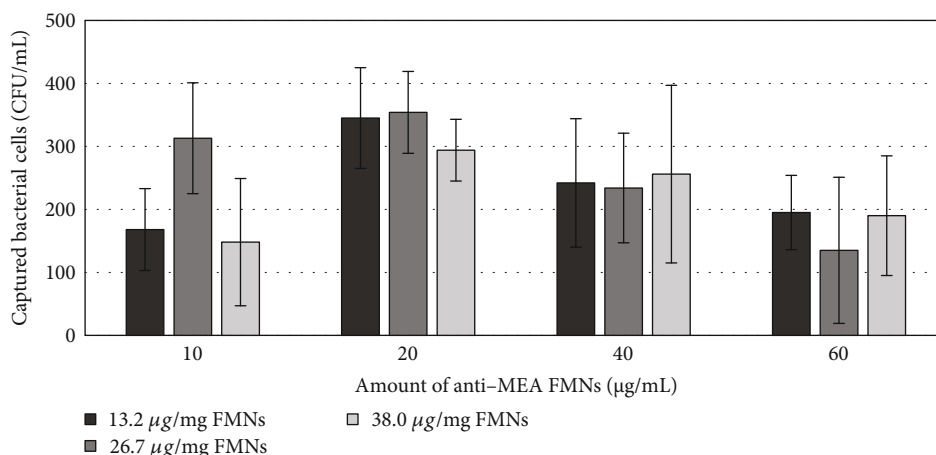
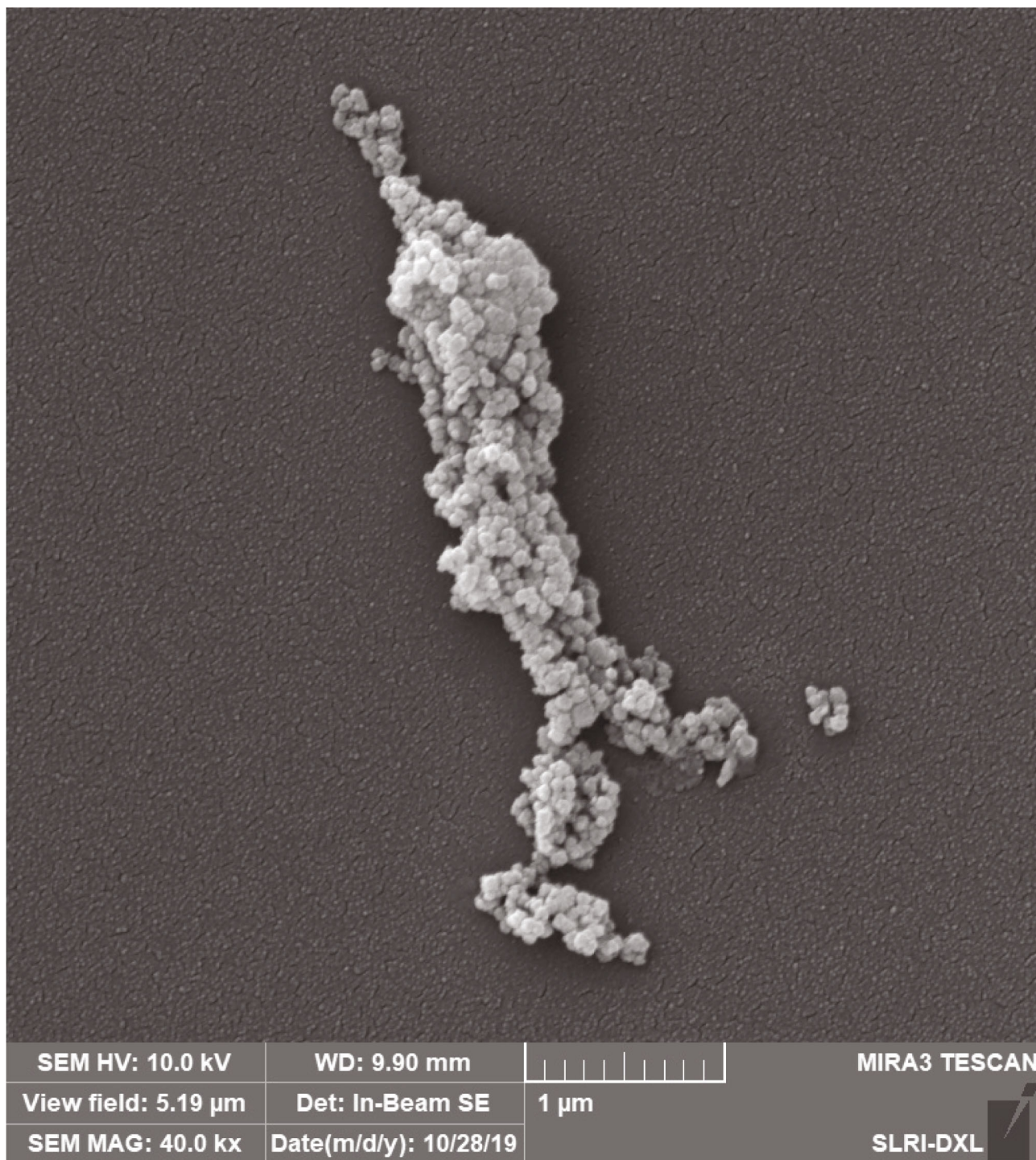


FIGURE 4: Optimization of amount of anti-MEA FMNs for capturing *C. jejuni* cells by IMS system.

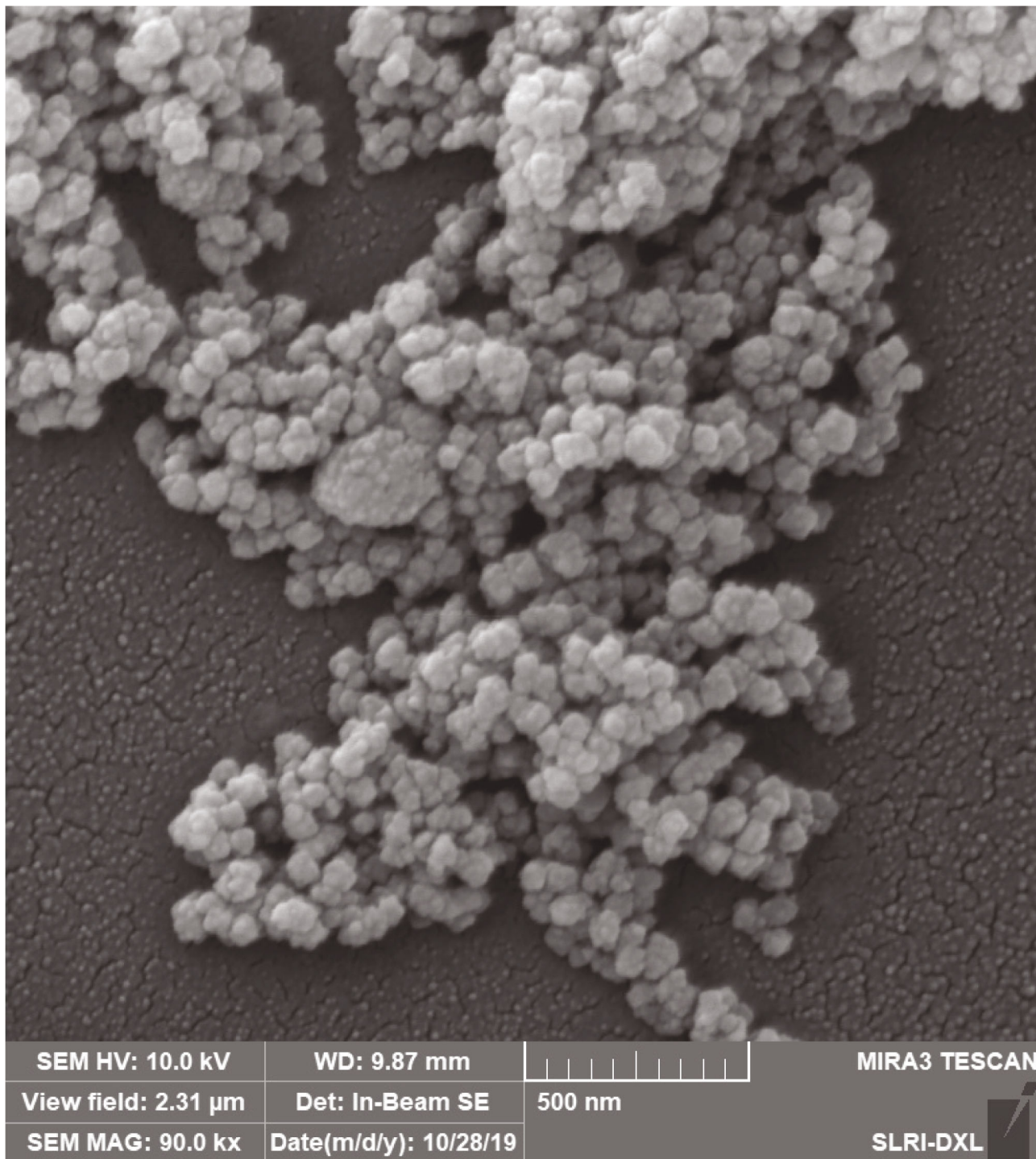
revealed that *C. jejuni* (Figure 5(c)) and *C. coli* (Figure 5(d)) cells were coated with high densities of anti-MEA FMNs, and single bacterial cells with FMNs appear to be aggregated into larger ellipse-like shapes. Similar aggregation phenomenon was also reported for VBNC *Vibrio parahaemolyticus*

using immunomagnetic separation and PMAxx-qPCR [40]. The functionalized FMNs were able to attach to *C. jejuni* cells via interaction between antigen binding site of anti-MEA pAb and the surface CadF antigen of both *C. jejuni* and *C. coli* [32]. However, *C. jejuni* cell was not fully



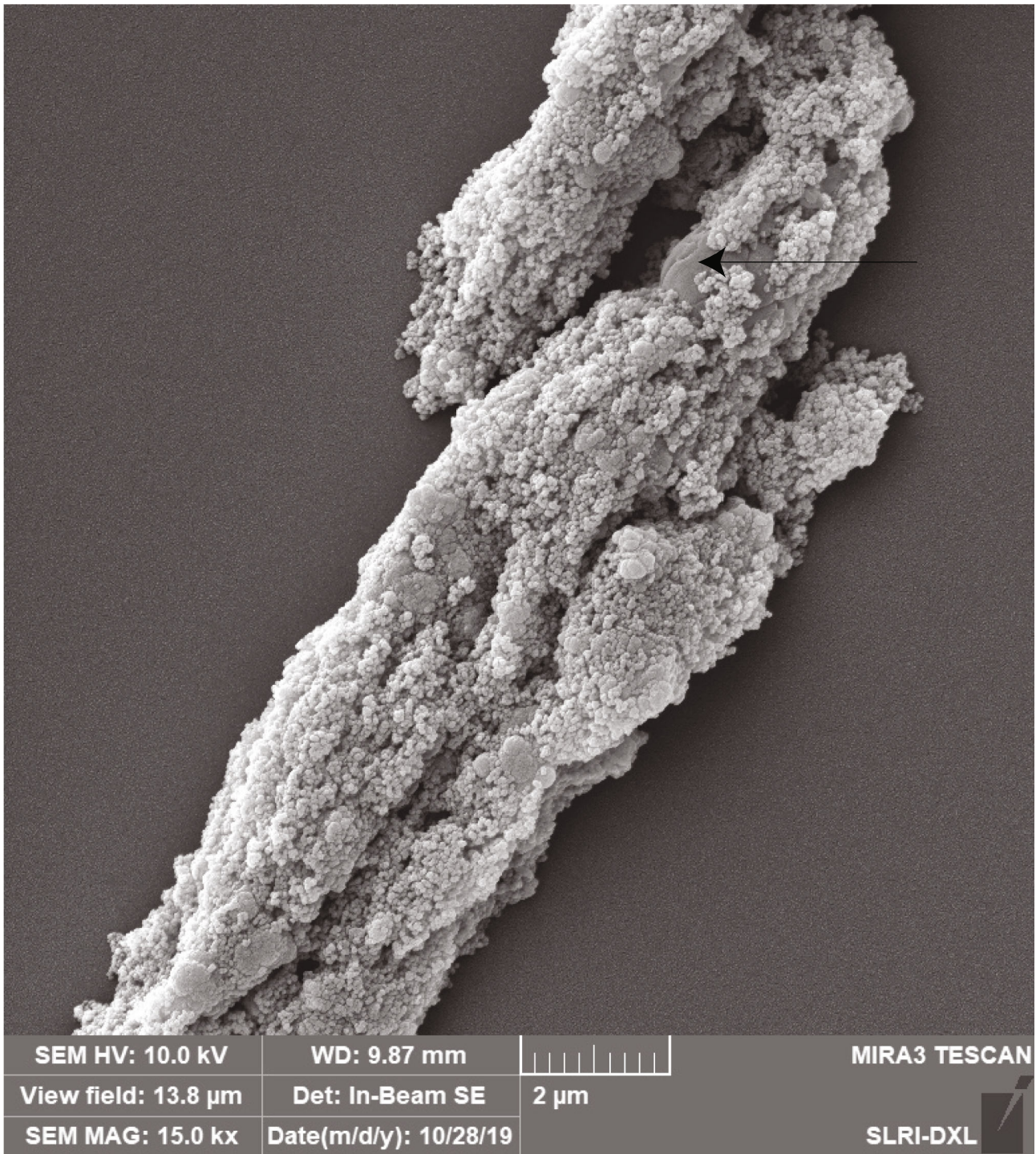
(a)

FIGURE 5: Continued.



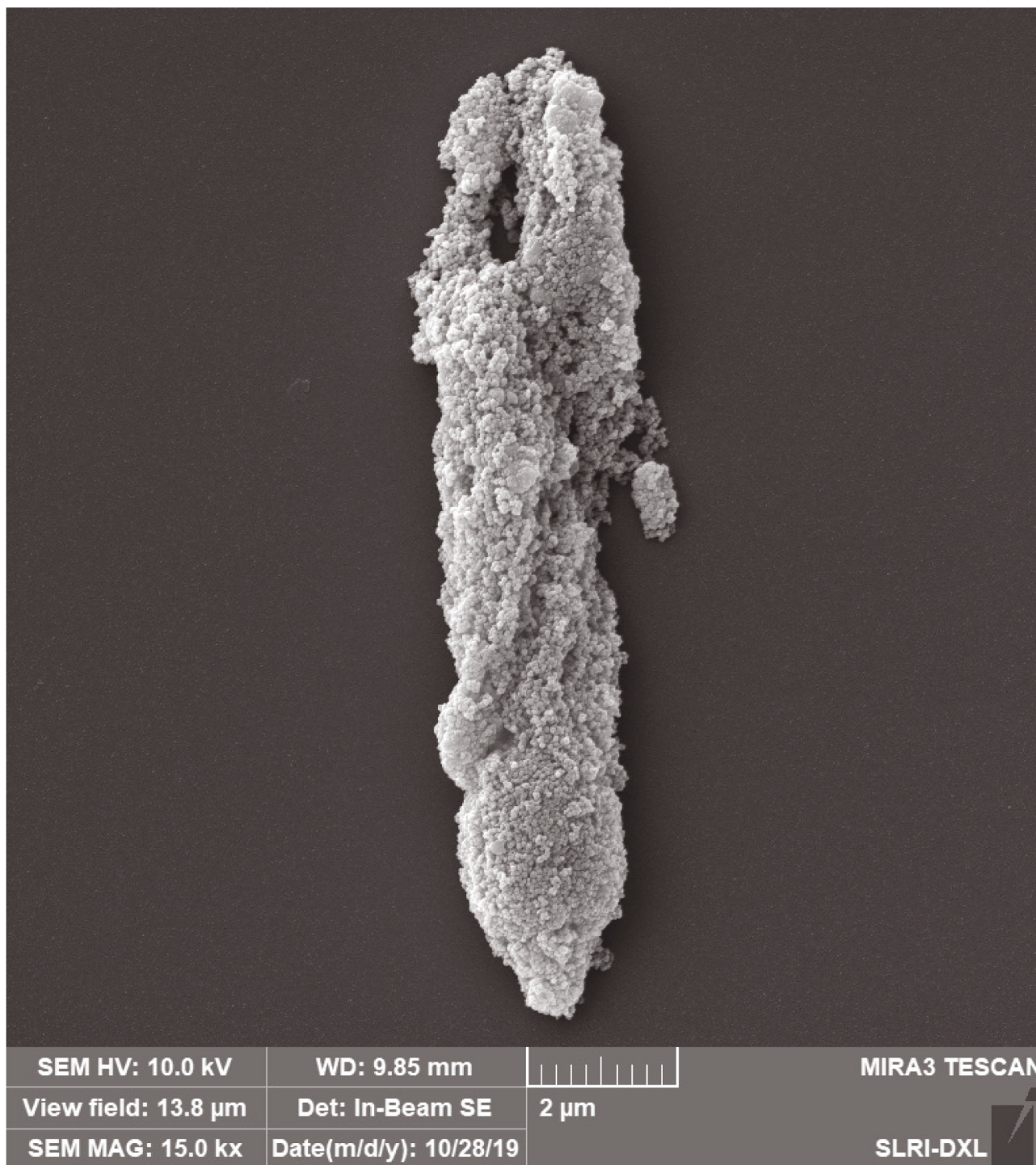
(b)

FIGURE 5: Continued.



(c)

FIGURE 5: Continued.



(d)

FIGURE 5: SEM images of anti-MEA FMNs at 40000 \times (a) and 90000 \times (b) magnification showing cube-like FMNs. The scale bars represent 1 μ m and 500 nm, respectively. Aggregation of bacterial cells surrounded with anti-MEA FMNs for *C. jejuni* (c) and *C. coli* (d) cells. Some small part of the cell surface was free from the anti-MEA FMNs, as indicated by an arrow. The bar represents 2 μ m.

covered by FMNs as certain parts of cell were free of FMNs (Figure 5(c)). These results confirmed that the anti-MEA pAb remained conjugated to FMNs and retained their immunological activities for binding to target cells.

3.5. *Optimization of Multiplex TD-PCR Assay.* Multiplex TD-PCR was next combined with the IMS technique for isolation and simultaneous detection of *C. jejuni* and *C. coli*. Primer pair (C412F-C1288R) targeting *16s rRNA* gene of

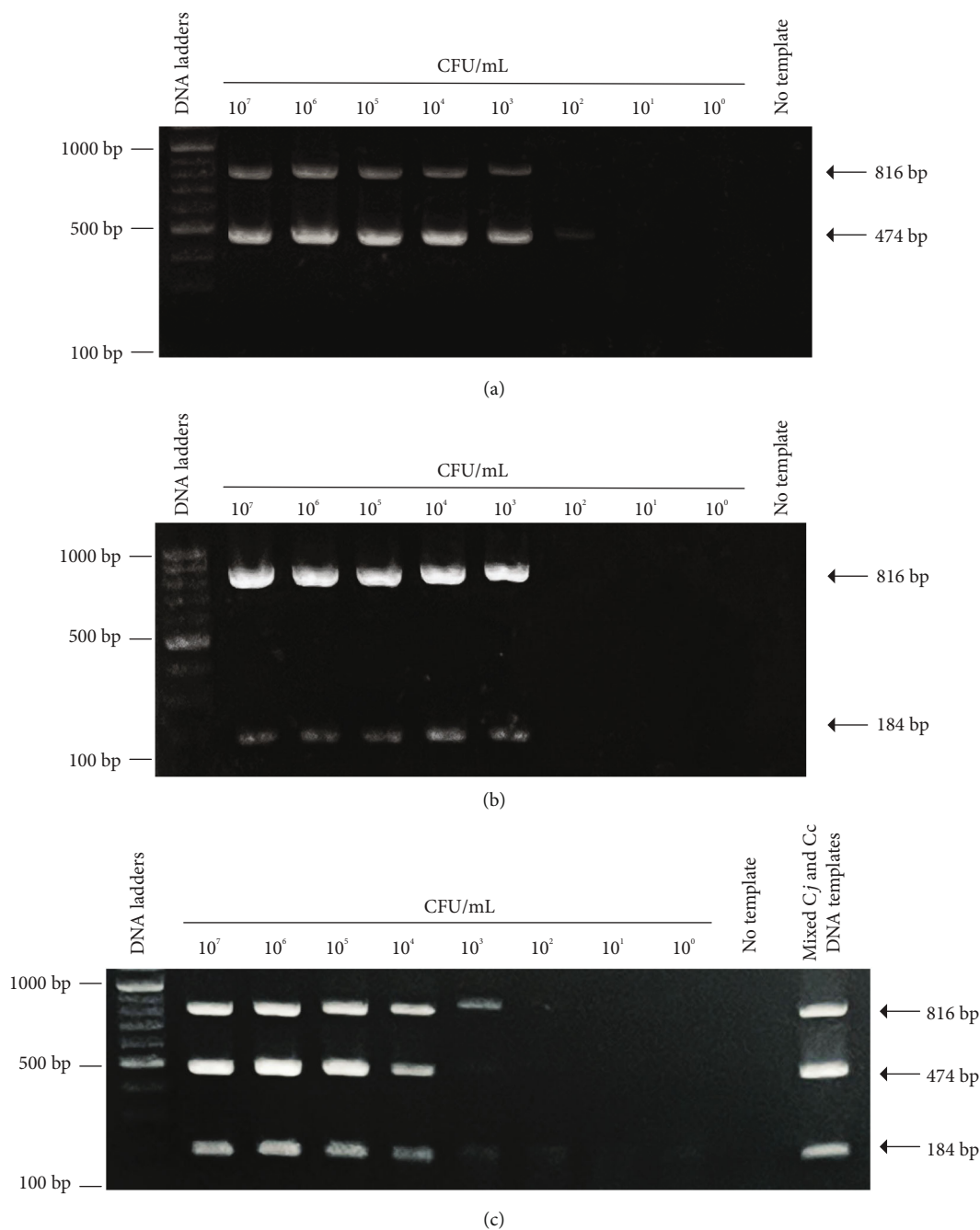


FIGURE 6: IMS-multiplex TD-PCR assays of single pure cultures of *C. jejuni* (a), *C. coli* (b), and mixed cultures (c). Negative control: no template lane; positive control: mixed *C. jejuni* and *C. coli* DNA templates.

Campylobacter spp. [38] was included in multiplex TD-PCR assay as a genus primer. For species identification, the other 2 primers, *hipO* gene-specific primer pair (FW226–RV699) and *ask* gene-specific primer (FW346–RV529) were used to amplify amplicons of 474 and 184 bp, respectively. Interestingly, multiplex TD-PCR assays using 3 primer pairs C412F–C1288R, FW226–RV699, and FW346–RV529 were successfully performed to simultaneously detect *C. jejuni* and *C. coli* in a single reaction. The optimal concentration of FW226 and RV699 was $0.3 \mu\text{M}$, yielding the highest intensity of PCR bands at 816, 474, and 184 bp from 16s

rRNA gene, *C. jejuni hipO* gene, and *C. coli ask* gene, respectively (Supplementary Figure S3).

HipO-specific PCR assays are widely used for identification of *C. jejuni* because of its uniqueness and high conservation among *C. jejuni* strains [44]. However, apart from the *hipO* gene, different specific genes are used for the molecular confirmation including the *cdtA*, *cdtB*, and *cdtC* gene cluster [45], oxidoreductase subunit-specific gene [46], *mapA* [47], and *lpxA* gene [48]. For identification of *C. coli*, the following genes have been used: *ceuE* [49, 50], *ask* [51], *glyA* [44], *lpxA* [48, 50], and *cdtA*, *cdtB*, and *cdtC*

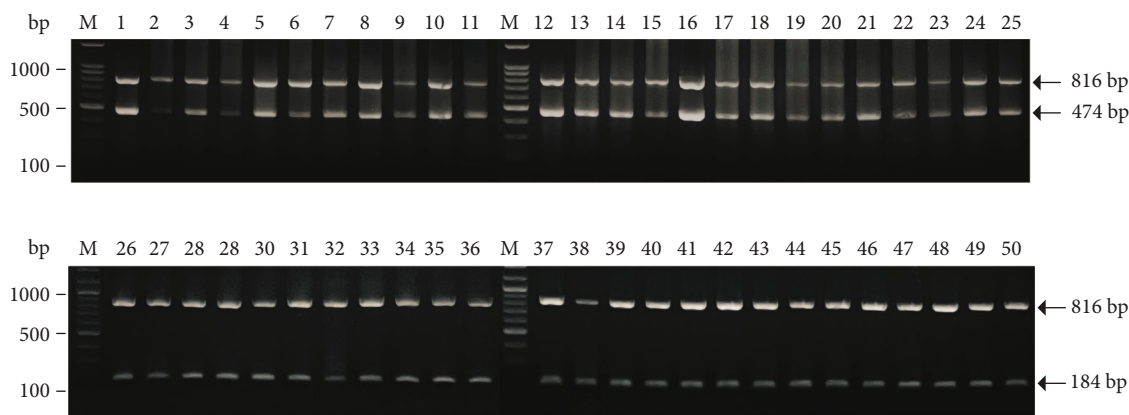


FIGURE 7: Inclusivity tested by IMS-multiplex TD-PCR assay. Lane M, DNA ladder; lanes 1-23, *C. jejuni* FSC strain No. 1-23; lanes 24-25, *C. jejuni* ATCC 33560 and DMST 29021, respectively; lanes 26-48, *C. coli* FSC strain No. 1-23; lanes 49-50, *C. coli* NTCC 11353 and DMST 28030, respectively.

TABLE 4: Inclusivity and exclusivity tests by IMS-multiplex TD-PCR assay.

Strains	Results		Total
	Positive (+)	Negative (-)	
Inclusivity ($n = 50$)			
<i>C. jejuni</i> (25) and <i>C. coli</i> (25)	50	0	50
Exclusivity ($n = 28$)	0	28	28
Total	50	28	78

gene cluster [45]. It was reported that using primer pairs specific to *C. jejuni* (*hipO*) and *C. coli* (*ask*) were unable to be conducted simultaneously in mPCR assay because there were differences in annealing temperature, time, and the number of PCR cycles [50]. However, *hipO* and *ask* gene-specific primers were successfully used in this study to detect and distinguish *C. jejuni* and *C. coli* in the multiplex TD-PCR.

3.6. Sensitivity of IMS-Multiplex TD-PCR Assays in Pure Culture Forms. *C. jejuni* and *C. coli* pure cultures were prepared at concentrations of 10^0 to 10^7 CFU/mL. For *C. jejuni*, the IMS-multiplex TD-PCR assays could detect amplicons of 816 bp and 474 bp from *16s rRNA* and *hipO* genes, respectively, at a concentration of 10^3 CFU/mL. However, only the PCR band of 474 bp was detected at 10^2 CFU/mL, as shown in Figure 6(a). In the same way, the specific DNA band of 184 bp for *C. coli* was detected at concentrations as low as 10^3 CFU/mL (Figure 6(b)).

For *C. jejuni* and *C. coli* mixtures at a cellular ratio of 1 : 1 and at all concentration levels, IMS-multiplex TD-PCR assay gave positive results from 10^4 to 10^7 CFU/mL where 3 corresponding amplicons were detected (Figure 6(c)). However, a weak band of amplicons could be detected at 10^3 CFU/mL. In addition, IMS-plating assays were performed to detect both target cells in the same set of mixed cultures. The IMS-plating assay detected target cells at an initial concentration of 10^5 CFU/mL (data not shown), while IMS-multiplex TD-PCR assay could detect 10^4 CFU/mL. The difference in LODs of IMS-multiplex TD-PCR and

IMS-plating assays was due to the fact that the plating assay only detects viable cells, but not dead or viable but nonculturable (VBNC) cells [52]. VBNC could be found in natural contaminated chicken carcasses at approximate range of 1.5 to 4 log CFU/g [53]. Nevertheless, this limitation is overcome by PCR-based detection, as it is able to detect nonculturable or nonviable cells after capture and IMS.

3.7. Specificity of IMS-Multiplex TD-PCR Assay. To study the specificity of IMS-multiplex TD-PCR assay, detection of a total of 50 inclusive isolates were tested by IMS-multiplex TD-PCR. All isolates were confirmed by biochemical and molecular methods to be *C. jejuni* ($n = 23$) and *C. coli* ($n = 23$) strains. Four reference strains of *C. jejuni* (ATCC 33560 and DMST 29021) and *C. coli* (NTCC 11353 and DMST 28030) were included in this study. Results of IMS-multiplex TD-PCR assay were positive for all inclusivity tests (Figure 7). The specificity was 100% for the *C. jejuni* and *C. coli* strains tested (Table 4).

The 28 isolates of exclusive strains were also tested by IMS-multiplex TD-PCR assays. As expected, negative results were received in all cases (100%) of exclusive isolates (Table 4) since none of specific amplified product were detected (Figure 8). The estimated CFU/mL of exclusive strains are determined by plating count and listed in supplementary Table S2. In addition, reference strains of *C. jejuni* ATCC 33560 and *C. coli* NTCC 11353 were randomly included in cocktails of exclusive strains. Similarly, specific amplicons were amplified selectively from target bacteria, as shown in Figure 8. The amplicon of 816 bp of *16s rRNA* gene was generated in all cocktails which indicated the presence of the *Campylobacter* genus. In the same way, amplicons of 474 and 184 bp were also detected for *C. jejuni* or *C. coli* for included cocktails, respectively. These studies indicate high specificity of the IMS-multiplex TD-PCR assay which could be utilized for detection of a wide range of *C. jejuni* and *C. coli* strains found in chicken samples.

3.8. Effect of Food Sample Matrices on IMS-Multiplex TD-PCR Assay and Its Sensitivity. Various types of immunomagnetic

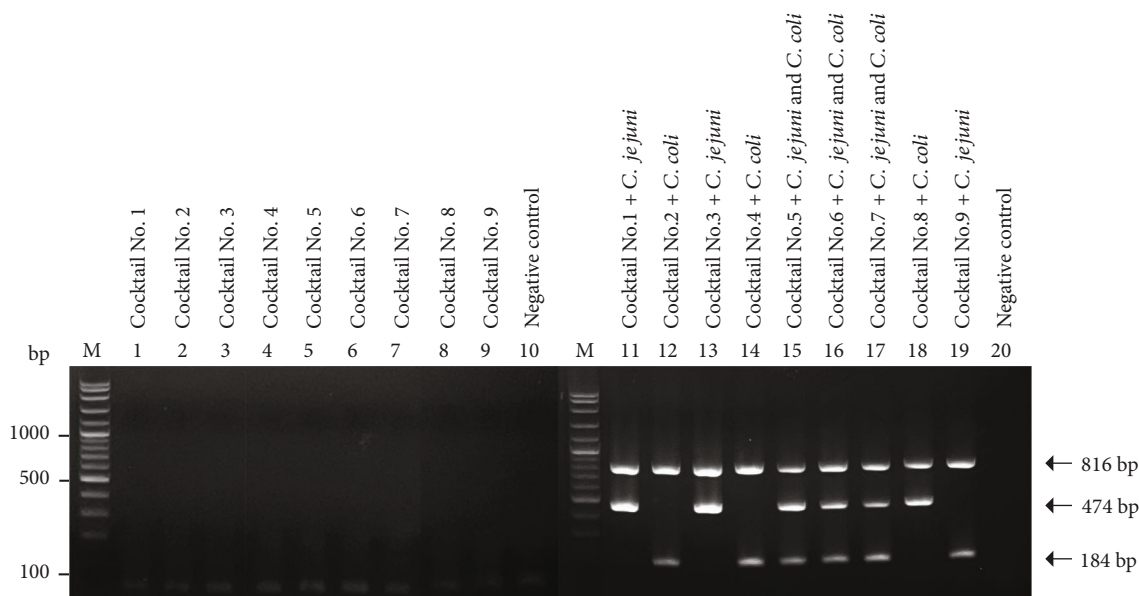


FIGURE 8: Exclusivity tested by IMS–multiplex TD–PCR assay. Lane M, DNA ladder; lanes 1–9, cocktail mixtures of exclusive strains No. 1–9; lanes 11–19, cocktail mixtures No. 1–9 with target bacteria, respectively; lanes 10 and 20, negative control (without DNA template). The cocktails of exclusive strains are listed in supplementary Table S2.

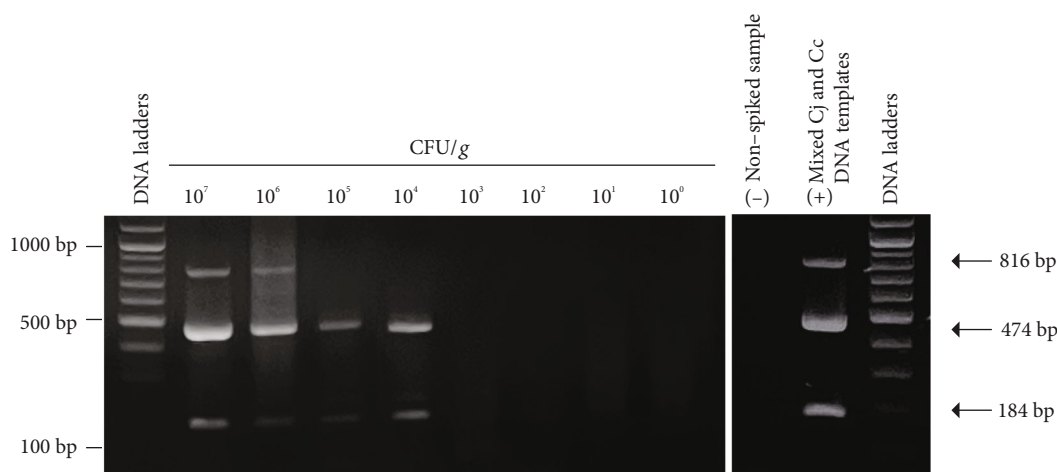


FIGURE 9: Detection *C. jejuni* and *C. coli* by IMS–multiplex TD–PCR assays of spiked chicken breast samples at different concentrations of mixed contamination (ratio 1 : 1) from 10^7 to 10^0 CFU/g. Lane, (-) negative control, and (+) positive control.

nanoparticles have been employed for capture of foodborne pathogens in biological samples including milk, beverages, and food matrices. Among poultry products, contamination of *Campylobacter* is frequently detected in chicken meat, especially chicken breasts [54]. Retail products of chicken meats have been reported with lower levels of contamination at 10^4 CFU per carcass [55]. IMS combined with PCR has previously been reported for detection *C. jejuni* in chicken fecal samples at 10^4 CFU/mL without enrichment [56]. In this study, natural chicken breast meat products that tested negative for *Campylobacter* with both conventional and IMS–multiplex TD–PCR assays were spiked with *Campylobacter* at different levels of contamination ranging from 1.2×10^0 to 1.2×10^7 CFU/g of chicken meat. The sensitivity of IMS–multiplex

TD–PCR assay was determined at 1.2×10^4 CFU/g for detection of both *C. jejuni* and *C. coli* (Figure 9), as there were two specific amplification products; a band of 816 bp from *16 s rRNA* gene was observed as low as 10^6 CFU/g. The IMS–multiplex TD–PCR assay was estimated to require 4 h of assay time.

The sensitivity and effectiveness of IMS combined with DNA–based assays (PCR and LAMP) rely on numerous factors [17]. Immobilization of antibodies onto FMNs with appropriate orientation such that active sites are displayed for target cells binding is a crucial factor. Inappropriate coupling could cause blocking of these active sites leading to a reduction of capture efficiency [17]. Sufficient DNA quality and quantity after extraction from captured cells are

additional important factors [42, 57]. Various DNA extraction methods have been used to extract genomic DNA from cells captured with immunomagnetic beads. Those methods include thermal or chemical treatments, boiling, and using commercial DNA extraction kits as well as combined methods. Some pretreatments have been used prior to DNA extraction. It has been reported that combination of lysozyme for cell lysis of *Listeria* sp. and use of ammonium acetate and glycogen in DNA extraction was more effective than only boiling and DNA extraction kits [57]. Poor quantity of extracted DNA could be caused by magnetic nanobeads. In this study, FMNs may cause in difficulty in DNA extraction because of a tight attachment between the particles and target cell. FMNs with smaller size of 72 nm could fully attach to entire target cell and tightly form aggregates or complexes. This phenomenon has been reported with magnetic beads of 180 nm size [42]. For this reason, an elution method has been applied for treating complexes of magnetic beads and captured cells. Target bacteria were eluted from immunomagnetic beads into Gly-HCl at low pH (2.2) and neutralized with Tris-HCl (pH 8.5), and the cell pellet was resuspended in small volume of 1× TZ lysing solution where sodium azide is included to improve the DNA extraction by boiling [42, 58]. Generally, complexes of immunomagnetic beads and target cells were resuspended in small volumes (50–100 μ L) of nuclease-free water or TE (Tris-EDTA) buffer prior to DNA extraction. Higher numbers of captured cells could yield higher DNA concentrations. Similarly, low DNA concentration may be caused by small amounts of captured target cells. Additionally, resuspending with large volumes of water or buffer caused dilution of DNA. Generally, extracted DNA samples have been included in PCR reactions at volumes varying from 1 to 5 μ L according to PCR protocols. In other work, however, immunomagnetic beads with captured cells have been suspended in 5 μ L of water and directly included in LAMP detection methods without DNA extraction [19]. Therefore, these different DNA extraction methods may affect amplification efficiency and lead to differences assay sensitivity.

In addition, reduction in sensitivity of the IMS-multiplex TD-PCR assay may be caused by various factors. First, food matrices could interfere with the binding between anti-MEA FMNs and target bacterial cells in sample reaction. Biological macromolecules (proteins and lipids) may also block binding between the immunomagnetic beads and the target cell. The capture efficiency values from food samples spiked with *Salmonella* typhimurium are approximately 20% lower than those from pure culture in all incubation times [59]. Similarly, sensitivity of IMS-lateral flow test strip (LFT) assay was reduced from 10^1 to 10^2 CFU/mL when it was tested in chicken meat sample [18]. Second, multiplex detection of more than one target gene can lead to decreased sensitivity compared to uniplex PCR due to primer competition and dimer formation. For example, uniplex PCR detected *C. jejuni* as low as 7.3×10^1 cell copies in pure culture sample, while higher numbers of *C. jejuni* (7.3×10^3 cell copies) were detected by mPCR in a mixed culture sample of 3 target bacteria [60]. Alves et al. (2012) reported that an mPCR assay could detect at 10^4 CFU/mL of *C. jejuni* ATCC 33291 and *Salmonella* enteritidis in pure culture. In addition,

the developed method was combined with a 24-h culture-based enrichment step to provide reliable conditions for the detection of the pathogenic bacteria at 10^2 CFU/mL of *C. jejuni* in spiked chicken meat. The enrichment diluted inhibitory substances and nonviable cells, although the analysis time increased [61]. However, rapid methods have been developed to reduce steps and time of analysis. Rapid detection methods generally require assay times of ~3 h to detect either thermophilic *Campylobacter* sp. or *C. jejuni* only. Rapid detection methods that include an enrichment step require assay times between 24–48 h to allow for propagation of target bacteria to detectable levels. In this study, the time of the IMS-multiplex TD-PCR assay was comparable to nonenrichment methods (Table 1); however, the advantage is in the ability to simultaneously detect and distinguish *C. jejuni* and *C. coli*, which is significant for informing the clinical treatment of *Campylobacter* infections. As a nonenrichment rapid method, the LODs of the IMS-multiplex TD-PCR assay were consistent to that of TaqMan real-time PCR assays which have reported sensitivities in the range of 10^4 to 10^7 CFU/g of *C. jejuni* in spiked samples [62].

4. Conclusion

In this study, an IMS-multiplex TD-PCR assay has been developed to simultaneously detect and distinguish *C. jejuni* and *C. coli*. The anti-MEA FMNs were able to capture both *Campylobacter* species, and multiplex TD-PCR was used to successfully and simultaneously identify each at concentrations 10^4 CFU/mL in a mixed culture. The LOD of multiplex TD-PCR assay was 10^4 CFU/g in spiked chicken breast meat samples. This assay is simple, rapid (4 h), and 100% specific to both *C. jejuni* and *C. coli* and thus is a promising alternative method for direct detection and identification of *C. jejuni* and *C. coli* in contaminated raw and chicken products. The method can serve both for detection and epidemiological applications.

Data Availability

The data that support the finding of this study were included within the supplementary materials file.

Conflicts of Interest

The authors declare that there is no conflict of interest regarding the publication of this paper.

Acknowledgments

This work was supported by the Agricultural Research Development Agency (ARDA) (grant numbers CRP6205030800), and Pattarapong Wenbap was supported by the Petchra Pra Jom Klao Ph.D. Research Scholarship from King Mongkut's University of Technology Thonburi (KMUTT), Thailand. Ryan Hansen would like to acknowledge NSF CAREER Award #1944791.

Supplementary Materials

Supplementary Materials were additionally provided to support experiments, results, and discussion. (*Supplementary Materials*)

References

- [1] Efsa, “The European Union one health 2020 zoonoses report,” *European Food Safety Authority Journal*, vol. 19, no. 12, pp. 1–324, 2021.
- [2] L. C. Ray, J. P. Collins, P. M. Griffin et al., “Decreased incidence of infections caused by pathogens transmitted commonly through food during the COVID-19 pandemic — Foodborne Diseases Active Surveillance Network, 10 U.S. Sites, 2017–2020,” *Morbidity and Mortality Weekly Report*, vol. 70, no. 38, pp. 1332–1336, 2021.
- [3] R. E. Black, M. M. Levine, M. L. Clements, T. P. Hughes, and M. J. Blaser, “Experimental *Campylobacter jejuni* infection in humans,” *The Journal of Infectious Diseases*, vol. 157, no. 3, pp. 472–479, 1988.
- [4] Y. Hara-Kudo and K. Takatori, “Contamination level and ingestion dose of foodborne pathogens associated with infections,” *Epidemiology and Infection*, vol. 139, no. 10, pp. 1505–1510, 2011.
- [5] N. O. Kaakoush, N. Castano-Rodriguez, H. M. Mitchell, and S. I. M. Man, “Global epidemiology of *Campylobacter* infection,” *Clinical Microbiology Reviews*, vol. 28, no. 3, pp. 687–720, 2015.
- [6] A. van Belkum, B. Jacobs, E. van Beek et al., “Can *Campylobacter coli* induce Guillain-Barré syndrome?,” *European Journal of Clinical Microbiology & Infectious Diseases: Official Publication of the European Society of Clinical Microbiology*, vol. 28, no. 5, pp. 557–560, 2009.
- [7] P. Myintzaw, A. K. Jaiswal, and S. Jaiswal, “A review on campylobacteriosis associated with poultry meat consumption,” *Food Reviews International*, pp. 1–15, 2021.
- [8] W. Samosornsuk, M. Asakura, E. Yoshida et al., “Isolation and characterization of *Campylobacter* strains from diarrheal patients in central and suburban Bangkok, Thailand,” *Japanese Journal of Infectious Diseases*, vol. 68, no. 3, pp. 209–215, 2015.
- [9] M. Shahbandeh, “Export Volume of Broiler Meat Worldwide in 2022, by Leading Country,” 2022, <https://www.statista.com/statistics/751000/export-of-poultry-meat-leading-exporter/>.
- [10] P. Prasertsri, “Thailand: Poultry and Products Annual,” 2021, <https://www.fas.usda.gov/data/thailand-poultry-and-products-annual-6>.
- [11] K. S. A. Kottawatta, M. A. P. Van Bergen, P. Abeynayake, J. A. Wagenaar, K. T. Veldman, and R. S. Kalupahana, “*Campylobacter* in broiler chicken and broiler meat in Sri Lanka: influence of semi-automated vs. wet market processing on *Campylobacter* contamination of broiler neck skin samples,” *Food*, vol. 6, no. 12, pp. 1–9, 2017.
- [12] L. García-Sánchez, B. Melero, I. Jaime, M.-L. Hänninen, M. Rossi, and J. Rovira, “*Campylobacter jejuni* survival in a poultry processing plant environment,” *Food Microbiology*, vol. 65, pp. 185–192, 2017.
- [13] Iso, “ISO 10272-1:2017 (EN) - Microbiology of the food chain horizontal method for detection and enumeration of *Campylobacter* spp,” p. 24, 2017.
- [14] S. C. Ricke, K. M. Feye, W. E. Chaney, Z. Shi, H. Pavlidis, and Y. Yang, “Developments in rapid detection methods for the detection of foodborne *Campylobacter* in the United States,” *Frontiers in Microbiology*, vol. 9, no. 3280, pp. 1–19, 2019.
- [15] N. R. Thornval and J. Hoorfar, “Progress in detection of *Campylobacter* in the food production chain,” *Current Opinion in Food Science*, vol. 39, pp. 16–21, 2021.
- [16] V. V. Mody, A. Singh, and B. Wesley, “Basics of magnetic nanoparticles for their application in the field of magnetic fluid hyperthermia,” *European Journal of Nanomedicine*, vol. 5, no. 1, pp. 11–21, 2013.
- [17] Z. Wang, R. Cai, Z. Gao, Y. Yuan, and T. Yue, “Immunomagnetic separation: an effective pretreatment technology for isolation and enrichment in food microorganisms detection,” *Comprehensive Reviews in Food Science and Food Safety*, vol. 19, no. 6, pp. 3802–3824, 2020.
- [18] W. Poonlapdecha, Y. Seetang-Nun, W. Wonglumsom et al., “Antibody-conjugated ferromagnetic nanoparticles with lateral flow test strip assay for rapid detection of *Campylobacter jejuni* in poultry samples,” *International Journal of Food Microbiology*, vol. 286, pp. 6–14, 2018.
- [19] M. R. Romero, M. D’Agostino, A. P. Arias et al., “An immunomagnetic separation/loop-mediated isothermal amplification method for rapid direct detection of thermotolerant *Campylobacter* spp. during poultry production,” *Journal of Applied Microbiology*, vol. 120, no. 2, pp. 469–477, 2016.
- [20] A. Kreitlow, A. Becker, M. F. Ahmed et al., “Combined loop-mediated isothermal amplification assays for rapid detection and one-step differentiation of *Campylobacter jejuni* and *Campylobacter coli* in meat products,” *Frontiers in Microbiology*, vol. 12, no. 1286, pp. 1–14, 2021.
- [21] P. Vizzini, M. Manzano, C. Farre et al., “Highly sensitive detection of *Campylobacter* spp. in chicken meat using a silica nanoparticle enhanced dot blot DNA biosensor,” *Biosensors & Bioelectronics*, vol. 171, pp. 1–9, 2021.
- [22] H. Asakura, J. Sakata, Y. Sasaki, and K. Kawatsu, “Development and evaluation of fluorescence immunochromatography for rapid and sensitive detection of thermophilic *Campylobacter*,” *Food Safety (Tokyo, Japan)*, vol. 9, no. 3, pp. 81–87, 2021.
- [23] A. C. Mulder, E. Franz, S. de Rijk et al., “Tracing the animal sources of surface water contamination with *Campylobacter jejuni* and *Campylobacter coli*,” *Water Research*, vol. 187, pp. 1–12, 2020.
- [24] A. Piccirillo, M. Giacomelli, G. Niero et al., “Multilocus sequence typing of *Campylobacter jejuni* and *Campylobacter coli* to identify potential sources of colonization in commercial Turkey farms,” *Avian Pathology*, vol. 47, no. 5, pp. 455–466, 2018.
- [25] M. E. Patrick, O. L. Henao, T. Robinson et al., “Features of illnesses caused by five species of *Campylobacter*, foodborne diseases active surveillance network (FoodNet) – 2010–2015,” *Epidemiology and Infection*, vol. 146, no. 1, pp. 1–10, 2018.
- [26] Y. S. Liao, B. H. Chen, R. H. Teng et al., “Antimicrobial resistance in *Campylobacter coli* and *Campylobacter jejuni* from human campylobacteriosis in Taiwan, 2016 to 2019,” *Antimicrobial Agents and Chemotherapy*, vol. 66, no. 1, pp. 1–14, 2022.
- [27] M. E. Konkel, S. G. Garvis, S. L. Tipton, D. E. Anderson, and W. Cieplak, “Identification and molecular cloning of a gene encoding a fibronectin-binding protein (*CadF*) from *Campylobacter jejuni*,” *Molecular Microbiology*, vol. 24, no. 5, pp. 953–963, 1997.

- [28] M. E. Konkel, A. G. Sean, J. K. Bong, G. G. Steven, and Y. Julie, "Identification of the enteropathogens *Campylobacter jejuni* and *Campylobacter coli* based on the *cadF* virulence gene and its product," *Journal of Clinical Microbiology*, vol. 37, no. 3, pp. 510–517, 1999.
- [29] M. Naseri, S. Shams, M. Moballeghe Naseri, and B. Bakhshi, "In silico analysis of epitope-based *CadF* vaccine design against *Campylobacter jejuni*," *BMC Research Notes*, vol. 13, no. 518, pp. 1–12, 2020.
- [30] M. E. Konkel, J. E. Christensen, A. M. Keech, M. R. Monteville, J. D. Klena, and S. G. Garvis, "Identification of a fibronectin-binding domain within the *Campylobacter jejuni* *CadF* protein," *Molecular Microbiology*, vol. 57, no. 4, pp. 1022–1035, 2005.
- [31] M. Krause-Gruszczynska, L. B. van Alphen, O. A. Oyarzabal et al., "Expression patterns and role of the *CadF* protein in *Campylobacter jejuni* and *Campylobacter coli*," *FEMS Microbiology Letters*, vol. 274, no. 1, pp. 9–16, 2007.
- [32] P. Wenbap, Y. Seetang-Nun, T. Luangtongkum, P. Khunrae, P. Tuitemwong, and T. Rattanarojpong, "Construction, expression and purification of a novel *CadF*-based multi-epitope antigen and its immunogenic polyclonal antibody specific to *Campylobacter jejuni* and *Campylobacter coli*," *Protein Expression and Purification*, vol. 180, article 105818, 2021.
- [33] N. Songvorawit, K. Tuitemwong, and P. Tuitemwong, "Single step synthesis of amino-functionalized magnetic nanoparticles with polyol technique at low temperature," *ISRN Nanotechnology*, vol. 2011, Article ID 483129, 6 pages, 2011.
- [34] K. A. Abd-Elsalam, "Bioinformatic tools and guideline for PCR primer design," *African Journal of Biotechnology*, vol. 2, no. 5, pp. 91–95, 2003.
- [35] National Center for Biotechnology Information, "U.S. National Library of Medicine (NCBI) Genbank Database," 2018, <https://www.ncbi.nlm.nih.gov/genbank/>.
- [36] Eurofins, "Genomics' Oligo Analysis Tool," 2018, <https://www.eurofinsgenomics.eu/en/ecom/tools/oligo-analysis/>.
- [37] National Center for Biotechnology Information, "U.S. National Library of Medicine (NCBI) Primer-BLAST," 2018, <https://www.ncbi.nlm.nih.gov/tools/primer-blast/>.
- [38] D. Linton, R. J. Owen, and J. Stanley, "Rapid identification by PCR of the genus *Campylobacter* and of five *Campylobacter* species enteropathogenic for man and animals," *Research in Microbiology*, vol. 147, no. 9, pp. 707–718, 1996.
- [39] J. Sukprasert, K. Thumanu, I. Phung-On et al., "Synchrotron FTIR light reveals signal changes of biofunctionalized magnetic nanoparticle attachment on *Salmonella* sp," *Journal of Nanomaterials*, vol. 2020, Article ID 6149713, 12 pages, 2020.
- [40] L. Zhao, X. Lv, X. Cao et al., "Improved quantitative detection of VBNC *Vibrio parahaemolyticus* using immunomagnetic separation and PMAxx-qPCR," *Food Control*, vol. 110, pp. 1–9, 2020.
- [41] J. Zhou, C. Zhang, X. Zhang et al., "Immunomagnetic separation-based nanogold enhanced surface plasmon resonance and colloidal gold test strips for rapid detection of *Vibrio parahaemolyticus*," *Archives of Microbiology*, vol. 202, no. 5, pp. 1025–1033, 2020.
- [42] Y. Bi, M. Shu, C. Zhong et al., "A novel SDS rinse and immunomagnetic beads separation combined with real-time loop-mediated isothermal amplification for rapid and sensitive detection of *Salmonella* in ready-to-eat duck meat," *Food Analytical Methods*, vol. 13, no. 5, pp. 1166–1175, 2020.
- [43] J. Chen and B. Park, "Effect of immunomagnetic bead size on recovery of foodborne pathogenic bacteria," *International Journal of Food Microbiology*, vol. 267, pp. 1–8, 2018.
- [44] G. Wang, C. G. Clark, T. M. Taylor et al., "Colony multiplex PCR assay for identification and differentiation of *Campylobacter jejuni*, *C. coli*, *C. lari*, *C. upsaliensis*, and *C. fetus* subsp. *fetus*," *Journal of Clinical Microbiology*, vol. 40, no. 12, pp. 4744–4747, 2002.
- [45] M. Asakura, W. Samosornsuk, M. Taguchi et al., "Comparative analysis of cytolethal distending toxin (*_cdt_*) genes among *_Campylobacter jejuni_*, *_C. coli_* and *_C. fetus_* strains," *Microbial Pathogenesis*, vol. 42, no. 5-6, pp. 174–183, 2007.
- [46] R. Nayak, T. M. Stewart, and M. S. Nawaz, "PCR identification of *_Campylobacter coli_* and *_Campylobacter jejuni_* by partial sequencing of virulence genes," *Molecular and Cellular Probes*, vol. 19, no. 3, pp. 187–193, 2005.
- [47] W. Müller, C. Böhlend, and U. Methner, "Detection and genotypic differentiation of *Campylobacter jejuni* and *Campylobacter coli* strains from laying hens by multiplex PCR and *fla*-typing," *Research in Veterinary Science*, vol. 91, no. 3, pp. 48–52, 2011.
- [48] J. D. Klena, C. T. Parker, K. Knibb et al., "Differentiation of *Campylobacter coli*, *Campylobacter jejuni*, *Campylobacter lari*, and *Campylobacter upsaliensis* by a multiplex PCR developed from the nucleotide sequence of the lipid *A* GenelpxA," *Journal of Clinical Microbiology*, vol. 42, no. 12, pp. 5549–5557, 2004.
- [49] I. Gonzalez, K. A. Grant, P. T. Richardson, S. F. Park, and M. D. Collins, "Specific identification of the enteropathogens *Campylobacter jejuni* and *Campylobacter coli* by using a PCR test based on the *ceuE* gene encoding a putative virulence determinant," *Journal of Clinical Microbiology*, vol. 35, no. 3, pp. 759–763, 1997.
- [50] S. M. L. Kabir, N. Chowdhury, M. Asakura et al., "Comparison of established PCR assays for accurate identification of *Campylobacter jejuni* and *Campylobacter coli*," *Japanese Journal of Infectious Diseases*, vol. 72, no. 2, pp. 81–87, 2019.
- [51] D. Linton, A. J. Lawson, R. J. Owen, and J. Stanley, "PCR detection, identification to species level, and fingerprinting of *Campylobacter jejuni* and *Campylobacter coli* direct from diarrheic samples," *Journal of Clinical Microbiology*, vol. 35, no. 10, pp. 2568–2572, 1997.
- [52] X. H. Zhao, J. L. Zhong, C. J. Wei, C. W. Lin, and T. Ding, "Current perspectives on viable but non-culturable state in foodborne pathogens," *Frontiers in Microbiology*, vol. 8, pp. 1–16, 2017.
- [53] A. Duarte, N. Botteldoorn, W. Coucke, S. Denayer, K. Dierick, and M. Uyttendaele, "Effect of exposure to stress conditions on propidium monoazide (PMA)-qPCR based *Campylobacter* enumeration in broiler carcass rinses," *Food Microbiology*, vol. 48, pp. 182–190, 2015.
- [54] H. Jribi, H. Sellami, S. Mariam et al., "Isolation and identification of *Campylobacter* spp. from poultry and poultry by-products in Tunisia by conventional culture method and multiplex real-time PCR," *Journal of Food Protection*, vol. 80, no. 10, pp. 1623–1627, 2017.
- [55] L. J. Walker, R. L. Wallace, J. J. Smith et al., "Prevalence of *Campylobacter coli* and *Campylobacter jejuni* in retail chicken, beef, lamb, and pork products in three Australian states," *Journal of Food Protection*, vol. 82, no. 12, pp. 2126–2134, 2019.
- [56] L. L. T. Tram, C. Cao, J. Høgberg, A. Wolff, and D. D. Bang, "Isolation and detection of *Campylobacter jejuni* from

- chicken fecal samples by immunomagnetic separation -PCR,” *Food Control*, vol. 24, no. 1-2, pp. 23–28, 2012.
- [57] Y. Mao, X. Huang, S. Xiong, H. Xu, Z. P. Aguilar, and Y. Xiong, “Large-volume immunomagnetic separation combined with multiplex PCR assay for simultaneous detection of *Listeria monocytogenes* and *Listeria ivanovii* in lettuce,” *Food Control*, vol. 59, pp. 601–608, 2016.
- [58] A. Abolmaaty, C. Vu, J. Oliver, and R. E. Levin, “Development of a new lysis solution for releasing genomic DNA from bacterial cells for DNA amplification by polymerase chain reaction,” *Microbios*, vol. 101, no. 400, pp. 181–189, 2000.
- [59] Q. Zheng, M. Mikg-Krajnik, Y. Yang, W. Xu, and H. G. Yuk, “Real-time PCR method combined with immunomagnetic separation for detecting healthy and heat-injured *Salmonella* Typhimurium on raw duck wings,” *International Journal of Food Microbiology*, vol. 186, pp. 6–13, 2014.
- [60] S. H. Park, I. Hanning, R. Jarquin et al., “Multiplex PCR assay for the detection and quantification of *Campylobacter* spp., *Escherichia coli* O157:H7, and *Salmonella* serotypes in water samples,” *FEMS Microbiology Letters*, vol. 316, no. 1, pp. 7–15, 2011.
- [61] J. Alves, V. V. Marques, L. F. P. Pereira, E. Y. Hirooka, and T. C. R. M. De Oliveira, “Multiplex PCR for the detection of *Campylobacter* spp. and *Salmonella* spp. in chicken meat,” *Journal of Food Safety*, vol. 32, no. 3, pp. 345–350, 2012.
- [62] Y. Liu, Y. Gao, T. Wang, Q. G. Dong, J. W. Li, and C. Niu, “Detection of 12 common food-borne bacterial pathogens by TaqMan real-time PCR using a single set of reaction conditions,” *Frontiers in Microbiology*, vol. 10, pp. 1–9, 2019.